MECSOL 2019 - Proceedings of the 7th International Symposium on Solid Mechanics,
V. Tita, A. Ferreira, M.L. Ribeiro, A. Vieira and A.T. Beck (Editors), ABCM, Sao Carlos, SP, Brazil, April 15th to 17th, 2019

Creep of filament wound composite rings under radial compression

Frederico Eggers[1], José Humberto S. Almeida Jr.[2], Cristiano B. de Azevedo[1], Sandro C. Amico[1]

[1]PPGE3M, Federal University of Rio Grande do Sul, Av. Bento Gonçalves 9500, 91501-970 Porto Alegre, RS, Brazil

[2]Mechanics and Composite Materials Department, Leibniz-Institut für Polymerforschung, Hohe Straße 6, 01069 Dresden, Germany

Abstract: The use of fiber reinforced polymer composites in structural applications, especially when submitted to hygrothermal loads, requires a thorough knowledge of the behavior during the life in service. Due to the viscoelastic response and the manufacturing method the time dependent behavior is studied in carbon/epoxy rings manufactured by filament winding. Test specimens with different stacking sequences were tested for creep under constant radial load for periods of 240 h in three hygrothermal conditioning variations. Through the creep curves and experimental analyzes a modification in the stiffness and the behavior of the material was verified, showing that the properties were affected by the time and conditioning, especially when above the ambient temperature.

Keywords: creep, filament wound ring, hygrothermal conditioning, radial compression

INTRODUCTION

Carbon fiber reinforced polymer (CFRP) composite structures have been increasingly used in many engineering applications given their high specific stiffness and strength and high corrosion resistance (Almeida Jr. et al, 2018). Filament wound (FW) pipes are often used in fluid transportation, where the fluid may change the mechanical behavior of the pipe. Consequently, once the pipe is continuously and simultaneously under thermal, environmental and mechanical stresses, durability and environmental aspects are issues that should be accounted for in the design chain. When the structure is under moisture and temperature, the long-term behavior of a CFRP may be affected by physical (e.g. changing in glass transition temperature - T_g) and chemical aging (change in molecular weight, oxidation). Some of the hygrothermal aging effects are reversible, such as the effect on T_g (may be reversible), and others are not, such as the plasticization of the matrix (Almeida Jr. et al, 2016).

In fact, swelling, plasticization and the slow hydrolysis of the polymeric matrix, and the slow attack of the liquid to the fiber/matrix interface correspond to the loss of properties which influence the durability of the structure. Given these reasons, the understanding of the long-term mechanical response of a CFRP structure under thermomechanical load taking into account environmental effects must be thoroughly investigated, once it may represent the real loading scenario of the structure (Guedes, 2018).

Creep refers to a time-dependent deformation under a constant load at a particular temperature. It is considered a crucial material property at a long-term point of view (Faraz et al, 2015). For composites, creep resistance is directly associated with the viscoelastic strain and fiber/matrix interfacial behavior (Almeida Jr. et al, 2018). Hence, these materials exhibit a time-dependent degradation in modulus (creep or stress relaxation) and strength (creep rupture) as a consequence of the viscoelasticity of the polymer matrix (Faria and Guedes, 2010).

Farshad and Necola, 2004 studied the effect of wet conditions on the long-term behavior of glass reinforced plastic (GRP) pipes with nominal diameter of 500 mm and length of 300 mm under water at room temperature in radial compression with constant dead weight. The experimental data were obtained over a period of 2 years and these data extrapolated to periods of up to 50 years. The test results show that strength of wet pipes after 1000 h was reduced to ≈60% compared to the dry pipe. Guedes et al, 2010 performed creep tests on GRP tubes having the same dimensions and loading conditions aforementioned. However, they determined the short and long-term rupture energies by evaluating the influence of preconditioning in water at 50 °C. They concluded that pre-conditioning reduced the initial stiffness and strength in ≈4% and ≈60%, respectively, considering a 50-year lifetime. Yang et al, 2018 evaluated the long-term creep behavior using time-temperature-stress superposition (TTSSP) principle and Findley model for CFRP tubes under bending. Creep tests were carried out at stress levels of 45%, 55%, 65%, and 75% of the ultimate flexural strength at constant temperatures ranging from −60 °C to 100 °C for 500 h. The tests indicated that creep rate increased with increasing stress and temperature levels, whereas the long-term deformation did not exceed the ultimate flexural strain, and the tube therefore met the required design requirements.

Considering that CFRP composite tubes are very stiff under normal operating conditions, their viscoelastic behavior is usually disregarded in structural designs. However, tubes wound at off-axis angles may, indeed, present a viscoelastic behavior, once both matrix and fiber/matrix interface might play a key role on the overall durability of the structure. In this context, the main focus of this study is to evaluate the creep response of carbon/epoxy filament wound rings under concomitant radial compression and hygrothermal conditioning. Furthermore, the influence of the winding angle is thoroughly evaluated.

EXPERIMETAL

Materials and manufacturing

The material used is a carbon/epoxy towpreg from TCR Composites, composed by a Toray T700-12K-50C carbon fiber reinforcement and UF3369 epoxy resin matrix. The tubes were manufactured via a filament winding machine using a KUKA 140 L100 robot. The design of the laminates was carried out via CadWind software.

Cylindrical tubes were manufactured onto a stainless-steel mandrel with 50.8 mm inner diameter and 1000 mm long. The following tubes were manufactured: [±60], [±75], [±90], [±60/±90] and [±75/±90], where a hoop layer has been added to the single-wall families in order to evaluate the effect of adding this layer on top of the non-geodesic ones. The hoop layer was written [±90], but in fact means [±89.6]. The winding patterns for the [±60] and [±75] families were 1/1, which means one diamond around the circumference.

The composite was cured in an oven with air circulation for 5 h at 120 °C. After cured, the system was cooled down up to room temperature and the composite tube was removed from the mandrel. The tubes were then cut into rings of 50 mm long. It was used a diamond saw with water in the cutting disc. After cut off, the samples were polished for burr removal.

Design of the creep equipment

A creep testing equipment was especially designed and produced for carrying out this investigation. It consists of a sliding platform mounted inside a rectangular metallic structure (Fig. 1a). Linear bearing housings were mounted at the corners of the platform to be later attached to the vertical guides. The function of the bearings is to restrict lateral movements and facilitate vertical displacement, as well as to decrease friction.

The equipment was produced with square carbon steel profiles and the bottom plate and the platform in SAE 1020 carbon steel. The vertical guides were machined with SAE 1045 carbon steel bars. In order to have liquid storage functionality and the ability to sustain the hygrothermal tests, the sides were closed with polycarbonate plates. For protection against corrosive effects, the structure was subjected to surface treatments and electrostatic painting. The vertical guides were covered with chrome.

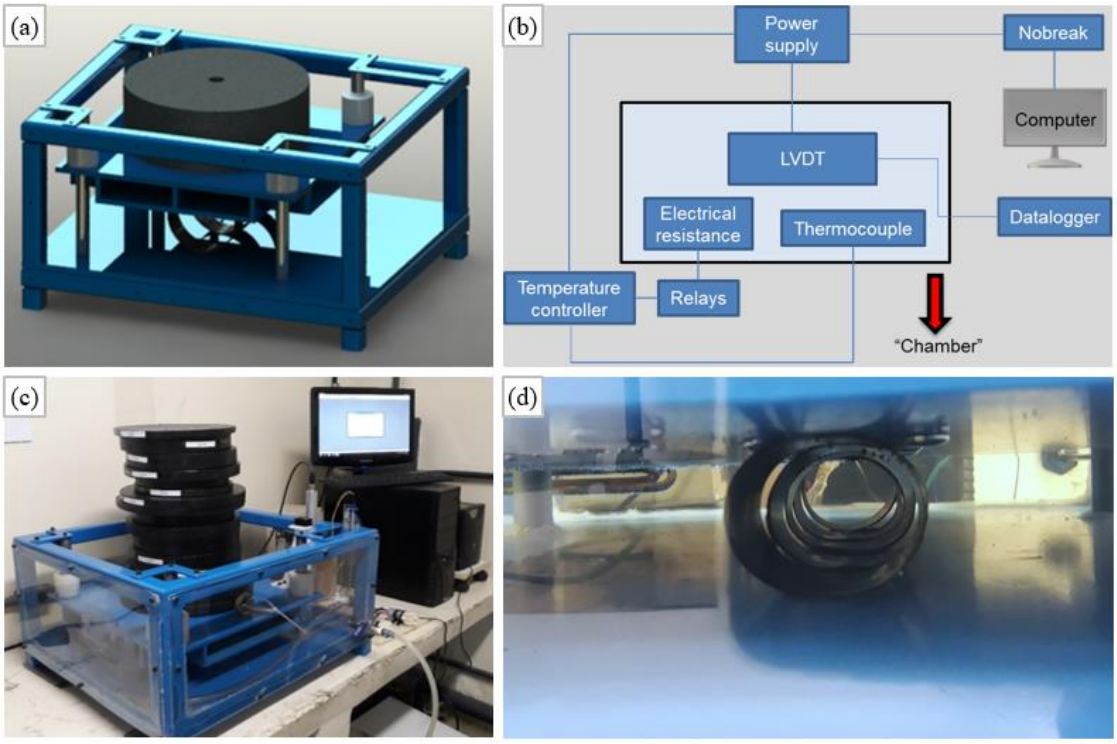

Figure 1 – Design of the creep testing equipment (a); schematics of the whole system (b); creep testing set up (c) specimens under creep loading (d).

In order to record the displacement of the specimens during the test, an instrumentation system has been assembled to the creep equipment (Fig. 1b). A tubular immersion electric resistance of 1500 W, a K-type thermoresistance, a Novus N480D digital temperature controller, a Balluff micropulse linear variable differential transformer (LVDT), a Novus Logbox AA data logger, a 24 V power supply, and a NHS no-break compose the whole system. The LVDT captures the displacement of the platform during the test. This sensor is fixed to the equipment and the magnet is bolted to the moving platform. When the platform shifts, an excitation is generated through a current pulse and this signal is processed and stored by the datalogger signal recorder, which transforms the data into displacement measurement and allows the instantaneous visualization on the computer screen through the software LogChart II.

For creep tests under hygrothermal conditioning and/or with hot water, a tubular electric resistance was installed inside the equipment. The temperature of the water is controlled by a digital controller that receives the thermoresistance information. In order to control the water level inside the "aquarium", a level sensor was assembled together with a mini pump. For water circulation, another mini pump was installed in closed cycle. To supply power to the system, a 24 V power supplier was used and a no-break was mounted.

Testing

Prior to the creep tests, quasi-static radial compressive tests (Fig. 2) were performed in an Instron Universal testing machine model 3382 in accordance with the recommendations of ASTM D2412-11 standard, at a speed of 2.5 mm/min. The experimental test concerns to the determination of the external load-deflection. Five samples free of burrs and jagged edges were tested. The objective was to evaluate the non-aged composites, determining the rupture loading and the stiffness of the “reference” composite rings.

Ring stiffness (RS), percentage ring deflection quota (P), and stiffness factor (SF) were calculated using Eqs. (1), (2) and (3), respectively. Once these values are highly dependent on the degree of deflection, changes in the radius of curvature occur. And the greater the deflection at which RS or SF are determined, the greater the magnitude of the deviation from the true value. Therefore, a correction factor ($C = (1 + \Delta y/2d)^3$) is applied to the RS and it is assumed that the ring will kept elliptical during the load application (Almeida Jr. et al, 2017).

$$RS = \frac{F}{\Delta_y}\left(1 + \frac{\Delta_y}{2d}\right)^3 \quad (1) \qquad P = \frac{\Delta_y}{d} \text{ x } 100\% \quad (2) \qquad SF = EI = 0.149r^3 \text{ x RS} \quad (3)$$

where: (F) is the applied load, (d) is the outside diameter and (Δ_y) is the change in the outside diameter of the specimen in the load direction. As reported by Almeida Jr. et al, 2017, the referred standard recommends that the change in inside diameter is used, however as the samples has different wall thicknesses, the outside diameter was used to provide more comprehensive results. For the stiffness factor, the EI variables represent the function of the flexural modulus (E) and the wall thickness (t) of the ring, since $I = t^3/12$. The variable (r) is the mid-wall radius, which is obtained by subtracting wall thickness from the outside diameter and dividing it by two.

Creep tests were performed under constant loading (Fig. 1c-d), which was 25% of the maximum compressive load of each family of laminates, where five samples were simultaneously subjected to radial compression at the same loading during 240 h (10 days). This period has been chosen because it is long enough to describe the viscoelastic behavior of the matrix, since the saturation is supposed to be reached at that time. The data acquisition was collected at a frequency of 0.05 Hz. Three scenarios have been considered: (i) only mechanical loading; (ii) mechanical loading and water immersion at room temperature; and (iii) with mechanical loading under water immersion at 40 °C.

The glass transition temperature (T_g) of the uncured towpreg and cured composite was measured through Differential Scanning Calorimetry (DSC) analysis using a DSC equipment model Q20 from TA Instruments.

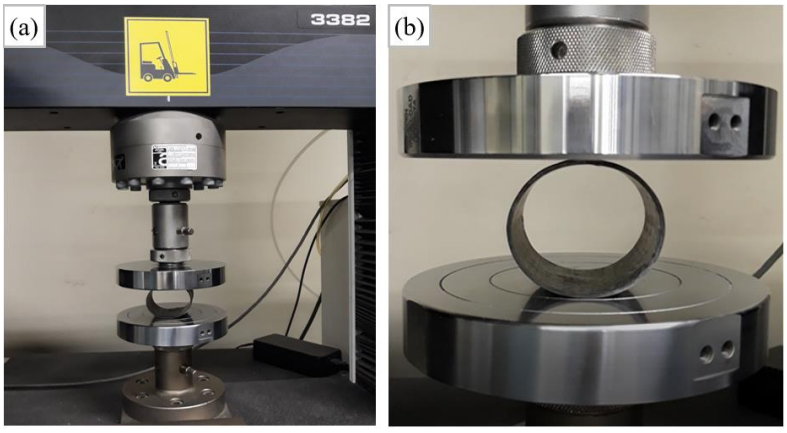

Figure 2 – Quasi-static radial compression test of a particular ring (a-b).

RESULTS AND DISCUSSION

To determine the curing degree of the prepreg, DSC analysis has been performed. Figure 3 presents DSC scans for un-cured prepreg and cured composites exposed to room temperature and after immersion in hot water at 40 °C for 240 h. It can be observed that for the uncured prepreg (1st heating), the crystallization process occurs, which is accompanied by latent heat release, thus generating a well-defined exothermic peak at approximately 165 °C. For the cured prepreg (2nd heating), the peak disappears and the T_g is of 97 °C. Thus, when comparing the DSC curves of the prepreg (2nd heating) and the unconditioned composite, an adequate degree of curing of the epoxy can be suggested due to the coincidence of the curves and the absence of crystallization peaks. Already for the wet-conditioned composite, the T_g decreases to 93 °C. There is also an intense drop in heat flow and a lack of curve stabilization. This effect is caused by the presence of moisture absorbed during immersion in water. De'Nève and Shanahan, 1993 concluded that a 1% of water uptake in epoxy resin corresponds to a reduction of 8 °C in T_g. Even in the case of exposure to room temperature, the water absorption in the free volume of the epoxy network can increase the chain mobility and an overall reduction in T_g (Dhieb et al, 2013). The decrease of glass transition by water absorption can be leads to can be increase the void and cracks as well as debonding between fiber and matrix (Kim and Takemura, 2011). And water temperature substantially affects the initial stiffness and viscoelastic behavior (Rafiee, 2016).

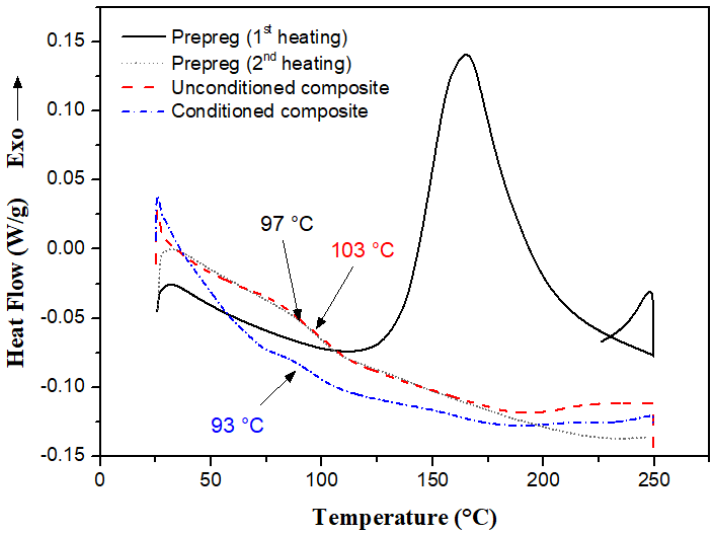

Figure 3 - DSC analysis of the rings before and after creep exposure in water at 40 °C for 240 h.

Figure 4a shows the load *vs.* deflection curves for all laminates under quasi-static radial compression. The higher the winding angle, the greater the maximum load carrying capacity, as expected, since the fibers are closer to the applied load. The maximum loads used to calculate the creep load for the laminates [±60], [±75], [±90], [±60/±90] and [±75/±90] were, 535, 713, 805, 1764 and 2239 N, respectively. Fig. 4b presents the stiffness of the composite rings and the rings with higher winding angles presented higher stiffness. When comparing the rings [±60] and [±90], the stiffness increase is of 56%, whereas comparing the samples with single layer [±60], in relation to the samples with additional hoop layer [±60/±90], the stiffness is 670% higher.

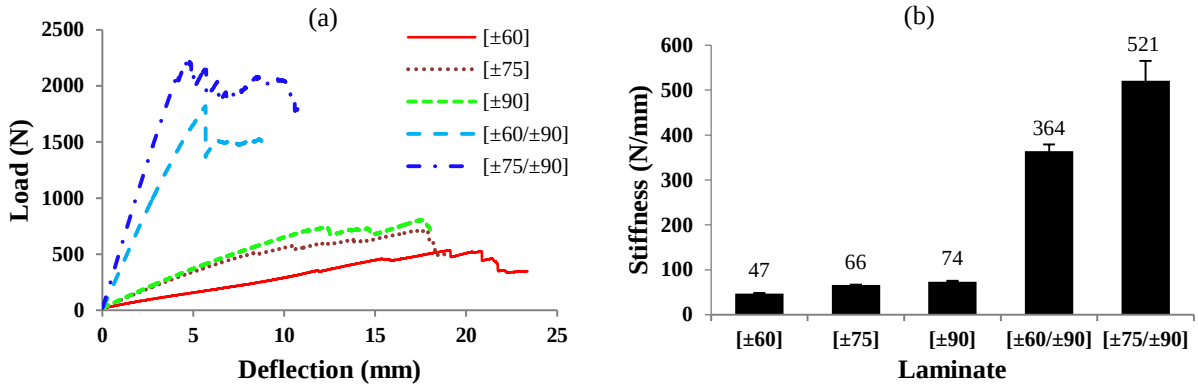

Figure 4 – Typical load *vs.* deflection curves (a) and stiffness for the rings under radial compression (b).

Figure 5 presents the creep curves for the composite rings subjected to radial compression under mechanical, hygro-mechanical and hygrothermal-mechanical conditioning. When comparing the behavior of the specimens subjected only to mechanical loading with samples mechanically loaded in water at room temperature, no significant changes have been observed. However, when creep tests are performed in hot water, the deflections are more significant. For example,

when comparing the results after 100 h of creep test in the conditions without water and with hot water, the increase in deflections were: 11.1%, 33.1%, 17.3%, 63.7% and 53.1% for the respective laminates [±60], [±75], [±90], [±60/±90], and [±75/±90]. An increase on the deflection in the intermediate phase of the loading in hot water is observed. This effect can be explained as a result of the thermal aging occurring in the matrix, thus reducing the stiffness of the rings.

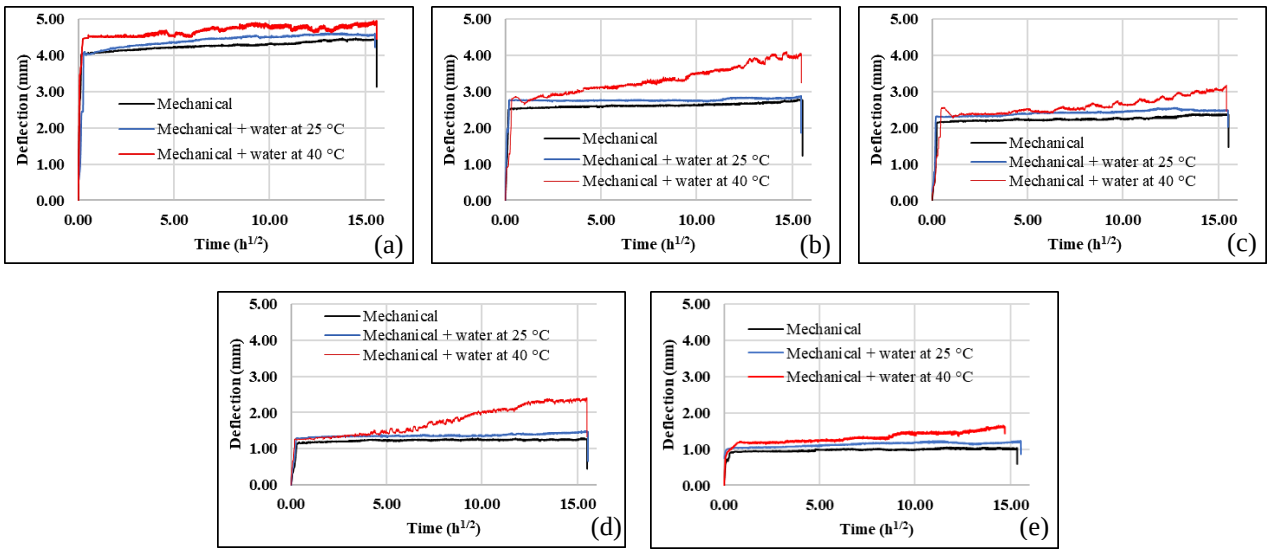

Figure 5 – Creep for the following laminates: [±60] (a); [±75] (b); [±90] (c); [±60/±90] (d); and [±75/±90] (e).

The residual properties of the composite rings are presented in Fig. 6 and Fig. 7, where "UC" refers to unconditioned, "ML" to mechanical loading, "ML+RTW" to mechanical loading and room temperature water, and "ML+HW" to mechanical loading and hot water.

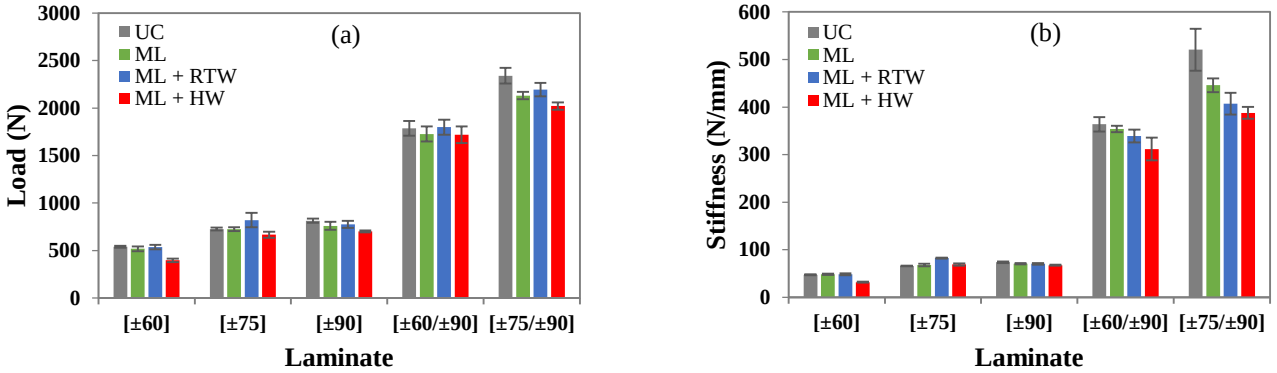

Figure 6 – Maximum load carrying capacity for the rings under radial compression (a); stiffness values of the studied rings (b).

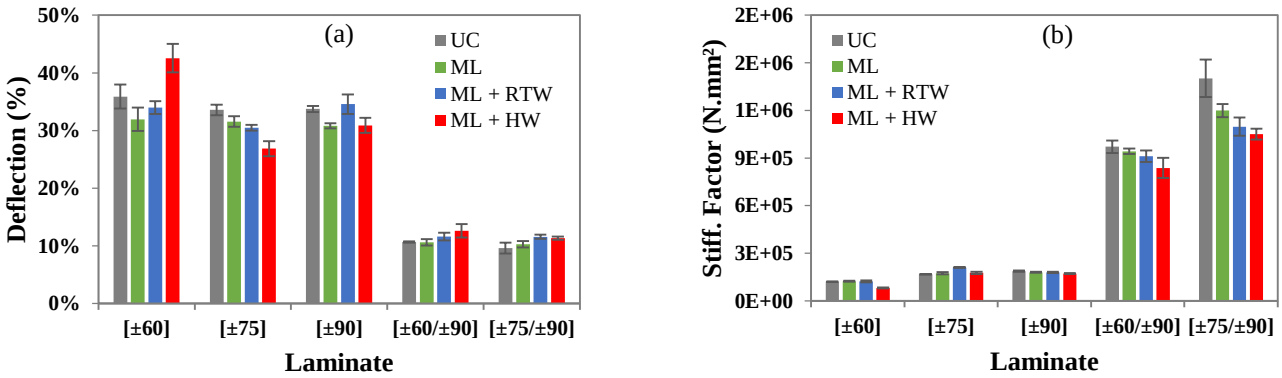

Figure 7 – Percentage deflection of the studied rings (a); Stiffness factor results for all rings (b).

Figure 6a shows the average maximum loads for each family. The results were obtained from the load *vs.* deflection for each ring under radial compression. For the composites submitted to the creep test these curves were not inserted in this work, however with some exceptions they followed the same tendency with the representative curves of Fig. 4a. Subtle load drops were observed in the final part of the loading until a rapid and intense failure, which is reported as the classical buckling behavior (Stedile Filho et al, 2018). The load reduction for composites [±90] and [±75/±90] when comparing the UC conditions with ML+HW was 14%. This decrease in load is recorded due to the deterioration process induced by the moisture of the materials, influencing the capacity to withstand higher loads (Jiang et al, 2014).

The stiffness results of the tested rings are shown in Fig. 6b. It is observed that the stiffness is influenced by the creep test and the loading conditions used, especially when carried out the test in an environment with water at 40 °C. The water diffusion and the thermal aging act on the degradation of the epoxy matrix, subsequently decreasing the mechanical strength (Almeida Jr. et al, 2016). For the rings [±75] and [±90], the stiffness showed no significant changes. As for the two-layer laminates, the stiffness decreased strongly when compared to the reference composites with the samples tested in hot water. This reduction was 14% and 26% for the rings [±60/±90] and [±75/±90], respectively. This corresponds to a residual stiffness of 86% of 364 N/mm and 74% of 521 N/mm.

Figure 7a shows the percentage of deflection of the rings. This parameter is associated with stiffness, and less stiff rings tend to deflect more. As the winding angle approaches the longitudinal axis and the diameter-to-thickness ratio increases, the load-bearing capacity decreases and the cross-section changes from a circle to an ellipse (Almeida Jr. et al, 2017). That is, the horizontal dimensions increase and in the vertical direction decrease. The biggest change usually occurs along the vertical direction. When the deflections are compared between the reference samples with the specimens that were submitted to the creep test, it is observed that for the single layer composites the deflection was reduced. This behavior can be justified by the test of creep and aging, which led to rupture of the material to occur before.

Figure 7b presents the stiffness factor for all rings, which is a useful design parameter related to flexural modulus and the wall thickness. And it is also highly dependent on the degree of deflection (Park et al, 2014). The stiffness factor follows the same trend of (RS), being higher for the rings with winding angle tending to [±90].

CONCLUSIONS

The focus of this study was the development of a creep testing equipment allowing hygro-thermomechanical conditioning to analyze long-term behavior of filament wound composite rings under radial compression. Composite rings with one ([±60], [±75] and [±90]) and two layers ([±60/±90] and [±75/±90]) have been manufactured and tested. Three conditions have been employed: only mechanical loading, hygro-mechanical loading and hygrothermal-mechanical loading. Then, creep tests during 240 h (10 days) were performed with a constant loading correspondent to 25% of the maximum radial compressive load. The results showed a strong influence of the thermomechanical conditioning on the ring deflection, where the rings presented a higher deflection when under hot water and mechanical loading simultaneously. In this case, the stiffness of the rings was reduced in 15% when compared to unconditioned samples. DSC analyzes showed that the rings were properly cured and that the thermal aging considerably reduced the T_g, which was caused by the plasticization of the matrix and caused by water absorption.

At all, the creep equipment developed was successful and useful for determining the long-term behavior of composite structures. Furthermore, it can be concluded that the time-dependent properties should be accounted for in the design of CFRP structures with off-axis layers.

ACKNOWLEDGMENTS

F. Eggers, C.B. Azevedo and SC. Amico would like to thank CAPES, CNPq and FAPERGS; J.H.S. Almeida Jr. is grateful to CAPES and Alexander von Humboldt for the financial support.

REFERENCES

Almeida Jr., J.H.S., Lorandi, N.P., Bregolin, B.P., Ornaghi, Jr., H.L., Amico, S.C., 2018, “Creep and interfacial behavior of carbon fiber reinforced epoxy filament wound laminates”, Polymer Composites, *in press*.

Almeida Jr., J.H.S., Ribeiro, M.L, Tita, V., Amico, S.C., 2017, “Damage modeling for carbon fiber/epoxy filament wound composite tubes under radial compression”, Composite Structures, Vol. 160, pp 204-210.

Almeida Jr., J.H.S., Souza, S.D.B., Botelho, E.C. Amico, S.C., 2016, “Carbon fiber-reinforced epoxy filament-wound composite laminates exposed to hygrothermal conditioning”, Journal of Materials Science, Vol.51, pp. 4697-4708.

Almeida Jr., J.H.S., Tonatto, M.L.P., Ribeiro, M.L., Tita, V., Amico, S.C., 2018, “Buckling and post-buckling of filament wound composite tubes under axial compression: linear, nonlinear, damage and experimental analyses”, Composites Part B, Vol.159, pp. 227-239.

De’Nève, B., Shanahan, M.E.R., 1993, “Water absorption by an epoxy resin and its effect on the mechanical properties and infra-red spectra”, Polymer, Vol.34, No. 24, pp. 5099-5105.

Dhieb, H., Buijnsters, J.G., Eddoumy, F., Vázquez, L., Celis, J.P., 2013, "Surface and sub-surface degradation of unidirectional carbon fiber reinforced epoxy composites under dry and wet reciprocating sliding", Composites: Part A, Vol.55, pp. 53-62.

Faraz, M.I., Besseling, N.A.M., Korobko, A.V., Picken, S.J., 2015, "Characterization and modeling of creep behavior of a thermoset nanocomposite", Polymer Composites, Vol.36, pp. 322-329.

Faria, H. and Guedes, R.M., 2010, "Long-term behavior of GFRP pipes: Reducing the prediction test duration", Polymer Testing, Vol.29, pp. 337-345.

Farshad, M., Necola, A., 2004, "Effect of aqueous environment on the long-term behavior of glass fiber-reinforced plastic pipes", Polymer Testing, Vol.23, pp. 163-167.

Filho, P.S., Almeida Jr., J.H.S., Amico, S.C., 2018, "Carbon/epoxy filament wound composite drive shafts under torsion and compression", Journal of Composite Materials, Vol.52, No. 8, pp. 1103-1111.

Guedes, R.M., 2018, "A systematic methodology for creep master curve construction using the stepped isostress method (SSM): a numerical assessment", Mechanics of Time-Dependent Materials, Vol. 22, pp. 79-93.

Guedes, R.M., Sá, A. and Faria, H., 2010, "On the prediction of long-term creep-failure of GRP pipes in aqueous environment", Polymer Composites, Vol.31, pp. 1047-1055.

Jiang, X., Kolstein, H., Bijlaard, F., Qiang, X., 2014, "Effects of hygrothermal aging on glass-fibre reinforced polymer laminates and adhesive of FRP composite bridge: Moisture diffusion characteristics", Composites: Part A, Vol.57, pp. 49-58.

Kim, H., Takemura, K., 2011, "Influence of water absorption on creep behaviour of carbon fiber/epoxy laminates", Procedia Engineering, Vol.10, pp. 2731-2736.

Park, J.S., Hong, W.H., Lee, W., Park, J.H., Yoon, S.J., 2014 "Pipe stiffness prediction of buried GFRP flexible pipe", Polymers & Polymer Composites, Vol.22, No. 1, pp. 17-24.

Rafiee, R., 2016, "On the mechanical performance of glass-fibre-reinforced thermosetting-resin pipes: A review", Composite Structures, Vol.143, pp. 151-164.

Yang, Z., Wang, H., Ma, X., Shang, F., Ma, Y., Shao, Z., Hou, D., 2018, "Flexural creep tests and long-term mechanical behavior of fiber-reinforced polymeric composite tubes", Composite Structures, Vol.193, pp. 154-164.

RESPONSIBILITY NOTICE

The author(s) is (are) the only responsible for the printed material included in this paper.